Paper accepted for presentation at 2009 IEEE Bucharest Power Tech Conference, June 28th - July 2nd, Bucharest, Romania

Optimal Operation of a Microturbine Cluster with Partial-Load Efficiency and Emission Characterization

Adrian-Valentin Boicea, *Student Member, IEEE*, Gianfranco Chicco, *Senior Member, IEEE*, and Pierluigi Mancarella, *Member, IEEE*

Abstract – **This paper discusses optimal operation strategies of a cluster of microturbines (MTs) for electrical load-following applications. Cluster operation ensures higher operational flexibility, but raises the issue of taking into account the partial-load MT characteristics, in terms of energy efficiency and pollutant emissions. In particular, from experimental results the NO_x and CO emissions exhibit nonlinear and to some extent complementary trends at different partial-load levels. Hence, individual optimizations of fuel consumption and emission reduction are first carried out in this paper to show the conflicting nature of such objectives. Then, multi-objective optimization is performed to directly determine the best-known Pareto front. For this purpose, a procedure based on evolutionary programming is illustrated and applied to a practical case study. The results point out the degree of trade-off that can be sought when minimizing the local environmental impact of such distributed energy systems.**

Index Terms **— distributed generation, environmental impact assessment, evolutionary algorithms, microturbine, multi-objective optimization, Pareto front.**

I. Introduction

MICROTURBINES (MTs) are being increasingly adopted in urban areas, where quite stringent local air quality requirements may pose serious constraints to the technology selection and machine operation [1]. In this respect, natural-gas fed MTs generally show relatively low emissions of hazardous pollutants such as NO_x and CO at full load [2,3]. However, these emissions may worsen consistently at partial load, as confirmed by a number of experimental results (see for instance [4,5]), and even non-monotonic variations of the emissions with respect to the loading level are possible. A key characteristic of MTs is the possibility to be operated in *clusters*, allowing the setup of optimal *dispatch strategies* of the different units aimed at minimizing specified objective functions. For load-following applications, relevant control strategies could prove effective to limit the emissions from the MT cluster under different load configurations. From this point of view, recent literature is addressing environmental and economic optimization problems for both distributed and large-scale thermal systems [6-10].

This paper illustrates the formulation and solution of energy and environmental optimization problems for a cluster of MTs in electrical load-following operation (relevant, for instance, to microgrid applications). More specifically, a minimum fuel consumption objective encompasses at the same time the optimization of energy efficiency, CO_2 emissions and fuel costs, whereas the *local* environmental impact from the MT cluster is minimized with reference to NO_x and CO emissions. Starting from the results obtained by individually optimizing the various objective functions, the presence of possible conflicting solutions is investigated. If conflicting cases arise, a multi-objective optimization problem is formulated and solved to find the compromise solutions belonging to the Pareto front, which provides meaningful insights on the trade-off to be sought by the decision maker.

II. Microturbine Performance

For the purpose of the analyses run in this paper, the energy performance of a MT unit is expressed by its *electrical efficiency* $\eta_W = W/F$, electrical energy output W [kWh_e] to fuel energy input F [kWh_t] ratio. MTs can in general cogenerate heat with high overall efficiency [11]; however, the focus of this paper is on electrical applications, and as such heat production is not considered.

In general, the electrical efficiency decreases at partial loads as a consequence of changes in the thermodynamic cycle characteristics. In addition, the worsening on the combustion characteristics usually brings about also an increase in pollutant emissions [12]. In some cases, emissions below 50% of the rated output become so high that the manufacturers themselves advice to switch the unit off.

The emission performance is characterized by using an *emission factor* model [2,3]. Following this approach, the mass emitted while producing the electrical energy output W is expressed as $m^p = \mu^p \cdot W$, with μ^p being the emission factor (specific emissions) of a given pollutant p, in [mg/kWh_e]). The emission factor depends on the technology and size of the unit, as well as on the operating conditions [2-4,13].

This work was in part supported by the Regione Piemonte, Torino, Italy, under the research grant C65/2004 "Territorial sustainability of distributed energy generation and interactions with electro-energetic systems".

A.-V. Boicea and G. Chicco are with Politecnico di Torino, Dipartimento di Ingegneria Elettrica, corso Duca degli Abruzzi 24, 10129 Torino, Italy (e-mail adrian-valentin.boicea@polito.it, gianfranco.chicco@polito.it).

P. Mancarella is with Imperial College London, Dept. of Electrical and Electronic Engineering, Exhibition Road, SW7 2AZ, London, UK (e-mail: p.mancarella@imperial.ac.uk).

978-1-4244-2235-7/09/$25.00 ©2009 IEEE

III. Multi-Objective Operational Optimization of Energy Efficiency and Emission Impact

Let us consider a given hourly electrical load energy W_{TOT} [kWh_e] to be supplied by a cluster of MT units operating in electrical load-following mode. The optimal share of the electrical load among the units can be determined by setting up a suitable optimization problem. Let us consider the following objectives to minimize:

- *Fuel consumption*, representing the energy efficiency goal. In economic terms, this also corresponds to minimization of the costs incurred to purchase the fuel. In addition, assuming that all MT units adopt the same fuel (*i.e.*, natural gas), fuel consumption minimization approximately corresponds to *CO_2 emission* minimization, according to the concepts discussed in [1,12]. The relevant aspect here is that, for a given W_{TOT}, energy efficiency, costs and CO_2 are deemed to be non-conflicting objectives under the hypotheses considered in this paper.
- *NO_x emissions*, being NO_x the most hazardous pollutant for equipment fed by natural gas [3,13], especially in urban areas subject to often stringent regulatory air quality constraints.
- *CO emissions*, typically very low at full load, but drastically increasing because of incomplete combustion at partial loads, or in case of inaccurate maintenance, or with aging of the components.

This partitioning of the objectives is done under the assumption that NO_x emissions, CO emissions and fuel consumption are conflicting objectives, as discussed with numerical evidence in the remainder of this paper.

The constraints applied to this problem are given by the energy balance between the MT generation and the total load, and by the operational limits of the equipment. The analyses carried out in this paper refer to the useful electrical output from the MTs. Thus, the *reference power* of each MT unit is obtained by subtracting from the rated power the amount of power needed to serve the auxiliary services of the unit (the gas compressor, in particular).

In mathematical terms, let us consider a cluster of $i = 1,\ldots, N$ MTs, each of which has a reference power $P_i^{(r)}$ [kW_e]. The loading level α_i of the i-th MT unit, for $i = 1,\ldots, N$, is expressed in relative values with respect to the reference power, and varies in the range [0;1]. Considering the minimum power $P_i^{(\min)}$ of the i-th unit, the constraint on the minimum loading of the MT unit is reflected on limiting the loading level within the range $[\alpha_i^{(\min)};1]$, where $\alpha_i^{(\min)} = P_i^{(\min)} / P_i^{(r)}$.

When operating at the loading level α_i, the i-th MT unit is characterized by electrical efficiency η_i, specific NO_x emissions $\mu_i^{NO_x}$ [mg/kWh_e], and specific CO emissions μ_i^{CO} [mg/kWh_e], for $i = 1,\ldots, N$. Considering a period $\tau = 1$ hour and a given hourly energy W_{TOT} supplied by the cluster of MTs to the load, the optimizations of the individual objectives are expressed as:

a) minimization of the fuel consumption:

$$\min \hat{f}^F(W_{TOT}) = \sum_{i=1}^{N} \frac{\alpha_i P_i^{(r)} \tau}{\eta_i} \quad (1)$$

b) minimization of the overall NO_x emissions:

$$\min \hat{f}^{NO_x}(W_{TOT}) = \sum_{i=1}^{N} \mu_i^{NO_x} \alpha_i P_i^{(r)} \tau \quad (2)$$

c) minimization of the overall CO emissions:

$$\min \hat{f}^{CO}(W_{TOT}) = \sum_{i=1}^{N} \mu_i^{CO} \alpha_i P_i^{(r)} \tau \quad (3)$$

The constraints are given by the energy balance

$$\sum_{i=1}^{N} \alpha_i P_i^{(r)} \tau - W_{TOT} = 0 \quad (4)$$

and by the loading level limits, for $i = 1,\ldots, N$:

$$\alpha_i \in \{0 \cup [\alpha_i^{(\min)};1]\} \quad (5)$$

For each objective $Z = \{F, NO_x, CO\}$, the above formulation is transformed into a penalized objective function, by considering the penalty factor γ applied to the energy balance constraint

$$f^Z(W_{TOT}) = \hat{f}^Z(W_{TOT}) - \gamma \cdot \left| \sum_{i=1}^{N} (\alpha_i P_i^{(r)} \tau) - W_{TOT} \right| \quad (6)$$

s.t. (5).

The optimization variables are the loading levels α_i, for $i = 1,\ldots, N$. Besides the non-connected loading level domain, the main challenges arising to compute the optimal solution depend on the non-linearity of the energy efficiency and emission characteristics, in the latter case with possible non-monotonic emission profiles at variable MT loading. These non-monotonic emission characteristics originate a non-convex search space. The various objective functions can be handled in two ways:

1. The individual optimization problems can be addressed separately. The optimization of the individual objective functions is carried out in this paper by using an *Evolutionary Algorithm* (EA) [14]. The MT unit data (power, efficiency and emissions) are coded by using a discrete number of points, representing the switch-off condition and a predefined number of discrete loading levels within the range $[\alpha_i^{(\min)};1]$. More details on the EA formulation and application are illustrated in Section IV.
2. The interactions among the various objectives can be dealt with under a comprehensive multi-objective optimization framework. In the presence of conflicting objectives, compromise solutions are obtained by constructing the *Pareto front*, composed of the *non-dominated* solutions for which it is not possible to improve the performance in one of the objectives without affecting another objective in an adverse way. The identification of the entire Pareto front for multi-objective combinatorial optimization problems is practically infeasible [15]. Thus, the aim of the computational procedure is to obtain a *subset* of the Pareto front (also called *best-known Pareto front*), by directly calculating a number of non-dominated solutions. EA techniques are the most used in the literature for addressing this kind of problems [15,16]. The determination of the best-

known Pareto front is carried out in this paper by using a specific EA version adapted to solve multi-objective optimization problems. The specific features of the EA, able to operate with a population of solutions and to explore different regions of the search space (even in non-convex cases), are exploited to obtain multiple non-dominated solution in a single execution. More details on the EA version implemented here are provided in Section IV.

IV. Multi-Objective Operational Optimization Solution through Evolutionary Algorithms

The two types of multi-objective optimization problems introduced in the previous section have been solved by using specific EA programming tools. Indeed, notwithstanding the common EA basis, these tools are rather different in their scope and implementation.

A. Individual optimization

For the *individual optimization* problem, a classical EA version has been implemented. The input data at partial load are the NO_x and CO emission characteristics, and the MT efficiencies. In the information coding, the chromosome structure is formed by a number N of genes equal to the number of MTs. Each gene is defined by D discrete states, each of which represents a specific operating level. The level #1 is the switch-off condition. Other D-1 levels are defined in the range $\left[\alpha_i^{(\min)};1\right]$, for i = 1,…, N. To form the initial population of K chromosomes, random levels re assigned to the genes.

All the individual objective functions are positive-valued. Since the individual objectives have to be minimized, while the EA intrinsically solves a maximization problem, each chromosome is associated to a fitness (to be maximized) defined by using the inverse of the objective function; considering the m-th chromosome for the objective Z, its fitness is:

$$\psi_m^Z = \frac{1/f_m^Z(W_{TOT})}{\sum_{\nu=1}^{M} 1/f_\nu^Z(W_{TOT})} \tag{7}$$

The classical genetic operators (selection, crossover and mutation) are then applied to form the new population. The chromosome *selection* is carried out by using the biased roulette wheel mechanism, in which the chromosomes of the new population are randomly selected on the basis of their fitness values. Crossover is applied to pairs of chromosomes of the selected population, if a random number extracted from a uniform probability distribution in the range [0;1] is lower than the user-defined crossover probability p_C; for the pairs of chromosomes satisfying the condition $r < p_C$, crossover is performed at a randomly chosen position. *Mutation* is performed on a single gene, but its application is decided by using a two-step mechanism, based on a user-defined mutation probability p_M referred to a chromosome. Given a random number r extracted from a uniform probability distribution in the range [0;1], if for a chromosome the condition $r < p_M$ is satisfied, then a randomly chosen gene inside the chromosome is subject to mutation. The discrete loading level in that gene is changed into a different loading level randomly chosen within the domain of definition of the D loading levels.

The *elitist* variant of the EA is adopted in the implementation, in which one copy of the chromosome corresponding to the best fitness is reproduced in the successive population without being modified by the selection, crossover and mutation operators. The stop criterion is applied by terminating the iterative process when there is no improvement in the best fitness over a predefined threshold $\varepsilon > 0$ for a specified number H of successive iterations.

B. Pareto front construction

For a multi-objective problem with individual objectives conflicting with each other, it is necessary to establish a sound criterion to manage the trade-off among the possible solutions. For this purpose, it is possible to exploit the concept of *Pareto dominance* [17]. In this respect, a solution is considered to be *non-dominated* if none of the other solutions exhibits lower values of *all* the individual objective functions. The set of all the non-dominated points that can be defined for the multi-objective optimization problem forms the *Pareto front*. The solutions located on the Pareto front contain the optimal points corresponding to the application of the individual optimization criteria, as well as a number of *compromise solutions* in which none of the individual optima is achieved.

The literature indicates a number of methods suitable for performing the *direct* construction of the *Pareto front*, or at least a portion of it, called the *best-known* Pareto front. Some of these methods have reached an acceptably good effectiveness in simultaneously finding out a number of compromise solutions [15,16,18].

In this paper, the multi-optimization problem to be solved is strongly affected by the presence of the equality constraint (4). As such, a custom EA-based computational program with specific arrangements has been written for determining the best-known Pareto front, rather than using existing programs. The basic difference with respect to the individual optimizations is the definition and use of the fitness in the EA application. In the Pareto front construction, higher fitness is assigned to the non-dominated points, and the genetic parameters in the EA are applied in such a way as to provide a suitable variety of search in the space of the possible combinations of the discrete loading levels that can be represented in the genes of each chromosome.

Fig. 1 shows a flow-chart of the computational procedure adopted. The global parameters are:

- the number K of chromosomes;
- the crossover probability p_C;
- the mutation probability p_M;
- the parameters L and ε used for the stop criterion;
- a method-specific parameter ζ used as a multiplier of the fitness values, as described in the sequel.

The chromosome coding for the K chromosomes is the same used for the individual optimization addressed in Section IV.A. The initial population is created at random. The fitness is initialized at unity for all the chromosomes. The individual objective functions are then calculated. On the basis of these objective functions, the non-dominated points are determined. The fitness is then updated by multiplying by ζ the fitness of the chromosomes corresponding to the non-dominated solutions. The global fitness is calculated as the sum of the fitness values. The stop criterion is then checked, according to

which the iterative process stops if no improvement in the global fitness over the threshold ε has been detected after L successive iterations. If the stop criterion is satisfied, then the non-dominated points are found, and the algorithm terminates with the output of the results. Conversely, a new population is created by applying the genetic operators of selection (through the biased roulette wheel, on the basis of the fitness of each chromosome), crossover and mutation (Section IV.A).

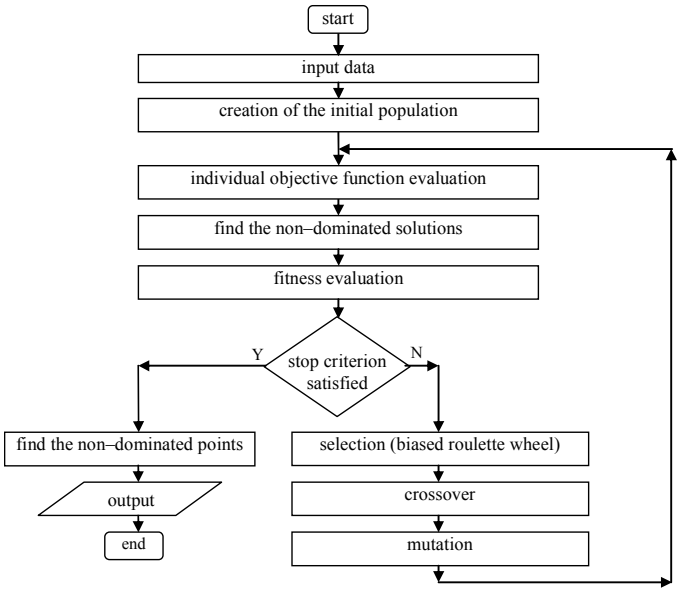

Fig. 1. Flow.chart of the EA-based procedure for determining the best-known Pareto front.

V. Case Study Applications

The optimizations illustrated in the previous sections are carried out on a cluster of 4 equal MTs. The MT used has 60 kW_e of rated capacity and with reference power of 55 kW_e (subtracting the power needed for the gas compressor operation, equal to about 5 kW_e and assumed to be constant at partial load for the sake of simplicity). The emission factors for the NO_x and CO pollutants are indicated in Fig. 2 for a sampled number of points elaborated from [4], relevant to experimental results at discrete steps of 1 kW_e. The efficiency values for the same set of sampled points are shown in Fig. 3.

A. Individual optimization results

Individual optimizations have been run for the various objective functions, considering different values of the total hourly energy W_{TOT} delivered to the electrical load [19].

In the EA application, the values of the parameters have been chosen after a number of preliminary tests, in order to balance the solution effectiveness and the computation time. The population is formed by K = 100 chromosomes, the crossover probability is p_C = 0.6, and the mutation probability p_M = 0.1. This mutation probability is relatively high with respect to common values used in other applications, in order to allow more frequent replacements of the discrete levels in the genes. The other parameters are the threshold ε = 0.1 (in order to verify the effective fitness improvement) and the limit L = 20 used in the stop criterion. The EA was not run in the cases in which the loading level was clearly met by a well-determined and intuitive combination of MT loading levels (such as for total load lower than the minimum loading level of a single MT or close to the sum of the reference powers of all the MTs).

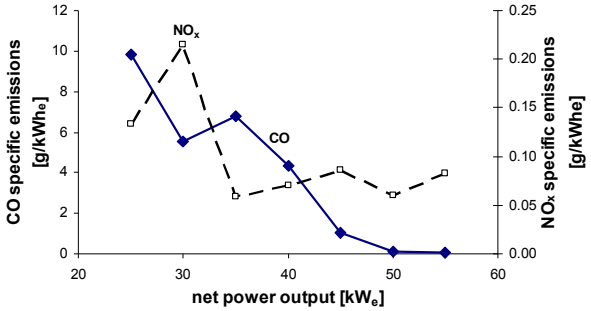

Fig. 2. NO_x and CO emission characteristics of the 60 kW_e MT.

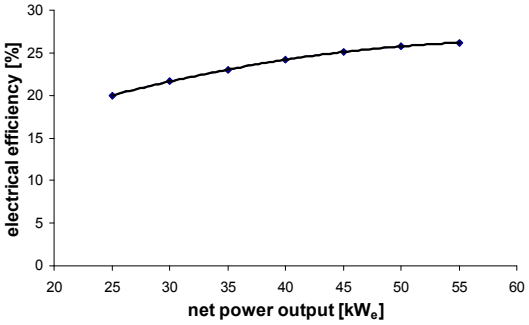

Fig. 3. Electrical efficiency of the 60 kW_e MT.

In the formation of the initial population, an additional criterion has been applied in this specific case with limited number of MTs, with the objective of increasing the number of initial chromosomes subject to null or small penalties in the penalized objective function (6). For this purpose, one half of the initial chromosomes chosen at random are accepted only if the corresponding total hourly energy does not differ more than 1% (in deficit or excess) with respect to W_{TOT}.

Fig. 4, Fig. 5 and Fig. 6 show the NO_x emissions, CO emissions and fuel consumption results, respectively, obtained with the three optimization objectives. Comparing the optimal and non-optimal results, the significant differences due to the effect of the opposite behaviour of NO_x and CO emissions in the intermediate partial-load operation region are quite evident. However, Fig. 6 shows no significant change in the fuel consumption from the different optimization strategies.

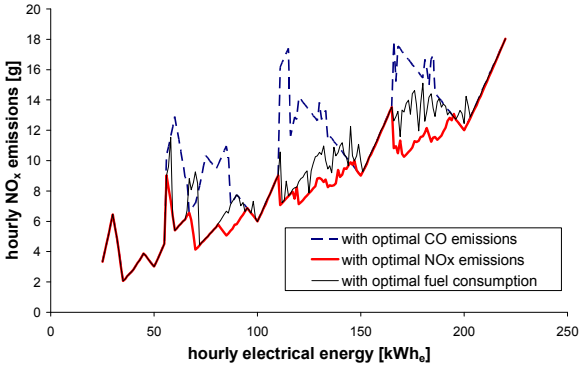

Fig. 4. NO_x emissions with different optimization objectives.

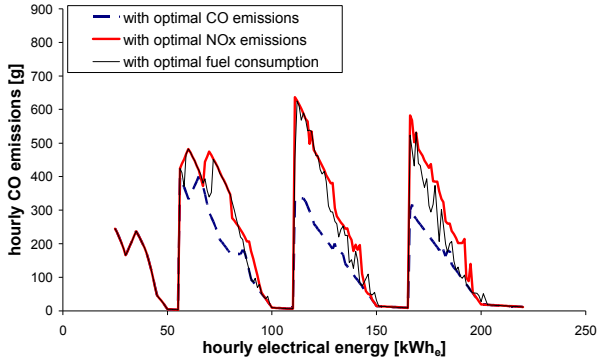

Fig. 5. CO emissions with different optimization objectives.

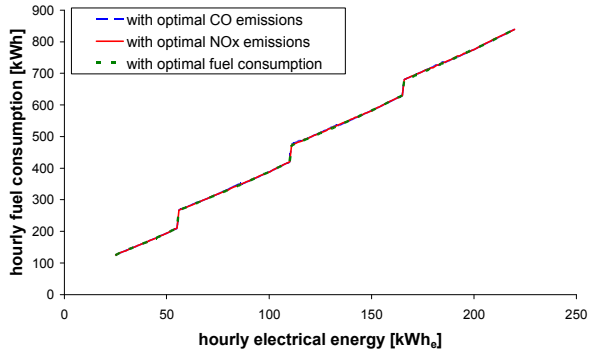

Fig. 6. Fuel consumption with different optimization objectives.

The *usage* of the MT units at the various hourly energy values is shown in Fig. 7 for minimum NO_x emissions, in Fig. 8 for the minimum CO emissions, and in Fig. 9 for the minimum fuel consumption.

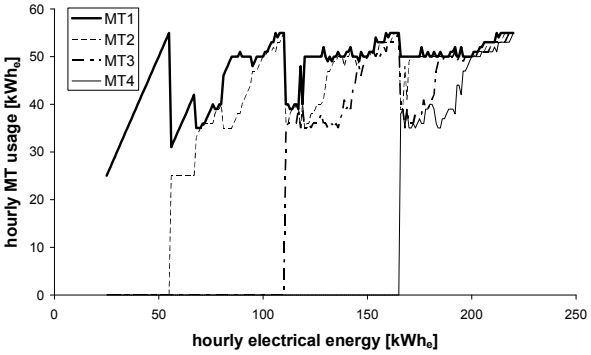

Fig. 7. MT usage with optimal NO_x emissions.

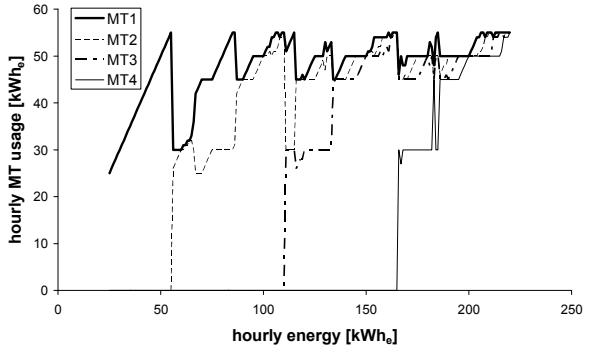

Fig. 8. MT usage with optimal CO emissions.

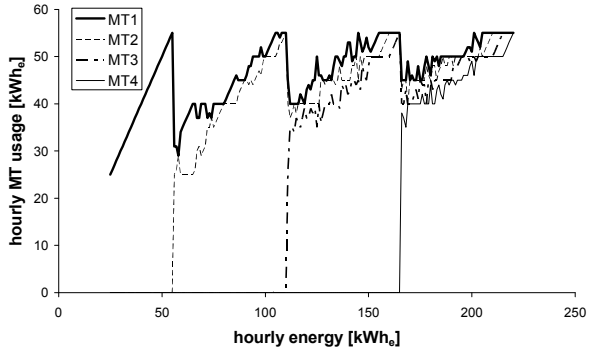

Fig. 9. MT usage with optimal fuel consumption.

Since the MT characteristics are equal, the attribution of the loading levels to each unit is arbitrary. For the sake of the representation, for each hourly energy, the loading levels in the optimal cases have been sorted in descending order, assigning the highest loading level to the unit MT1, the successive value in descending order to the unit MT2, and so forth. In practice, the operation schedule of the units has to be analysed by considering specific load patterns in the time domain (as in next section) and taking into account further operational limits (for instance, the number of switch on/off operations during the day, to avoid maintenance problems).

B. Application to a commercial centre

The individual optimization results are applied to an illustrative real case, referred to a commercial centre. The electrical load pattern data containing the total electricity consumption have been measured on the field, and are represented in sampled form at discrete time steps of 15 minutes each (Fig. 10). The electrical demand of the commercial centre is covered by using the cluster of $N = 4$ MTs addressed in the previous section.

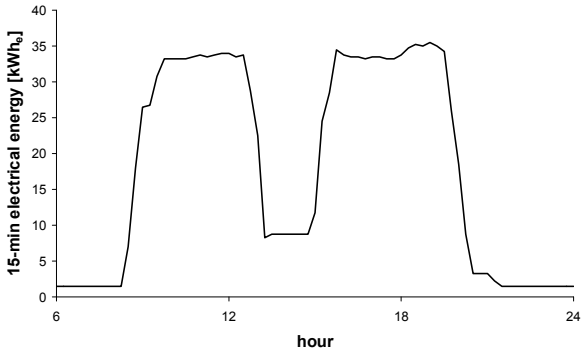

Fig. 10. Daily electrical load profile of the commercial centre.

Different patterns of electricity generation from the MTs are formed at each point in time, on the basis of the results found from the optimizations carried out by applying the different individual objectives. Fig. 11 shows the comparison among the 15-min NO_x emissions results. The NO_x emission pattern corresponding to the optimal CO results exhibits a large increase with respect to the one representing the optimal NO_x emissions, while the NO_x emission worsening obtained by using the minimum fuel consumption strategy is lower. This clearly depends on the different trends of NO_x and CO emissions, as already remarked. Indeed, with this example it is possible to give a quantification of this worsening in a real

situation. The daily NO_x emissions from the optimal NO_x strategy are 109 g. The increase in the daily NO_x emissions when using the other optimal strategies is significantly high, with 151 g (+39%) from the optimal CO emission results, and 132 g (+21%) from the optimal fuel consumption results.

Fig. 12 shows the comparison among the 15-min CO emissions results. The same type of considerations indicated above are valid to explain that the CO emission pattern corresponding to the optimal NO_x results exhibits a large increase with respect to the one representing the optimal CO emissions, while the CO emission worsening obtained by using the minimum fuel consumption strategy is lower. In quantitative terms, the daily CO emissions from the optimal CO strategy are 1986 g. Again, the increase in the daily CO emissions when using the other optimal strategies is significantly high, with 3532 g (+78%) from the optimal NO_x emission results, and 2800 g (+41%) from the optimal fuel consumption results.

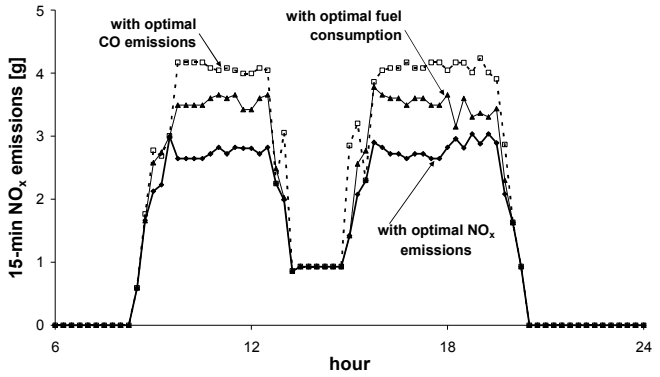

Fig. 11. NO_x emissions in the three optimization contexts.

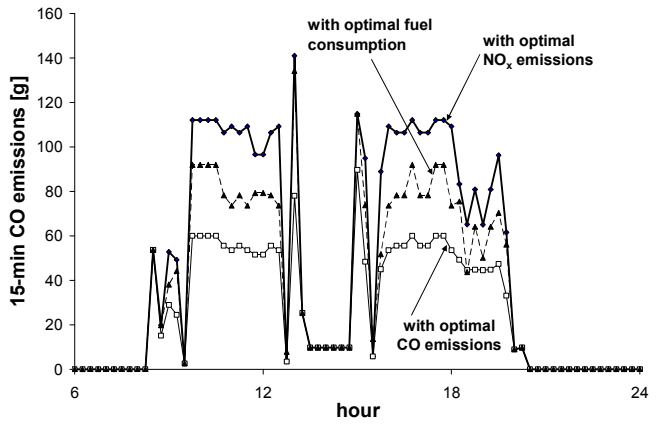

Fig. 12. CO emissions in the three optimization contexts.

Fig. 13 contains the 15-min fuel consumption patterns corresponding to the three optimization criteria. However, in this case the results are highly overlapped, and no significant difference is visible.

Possible *usage* patterns of the individual MT units are shown in Fig. 14 for the minimum NO_x emission case, in Fig. 15 for the minimum CO emission case, and in Fig. 16 for the minimum fuel consumption case. As it can be seen from these figures, it is possible to identify the usage patterns in such a way that the number of switch on/off transitions during the day is limited to one (for MT 1) or two times (for the other MTs). This allows reducing maintenance problems due to these transitions and guarantees better operational performance and longer lifetime of the MT units. Nevertheless, the usage patterns are different in the various cases, being more similar to each other when fuel consumption is minimized.

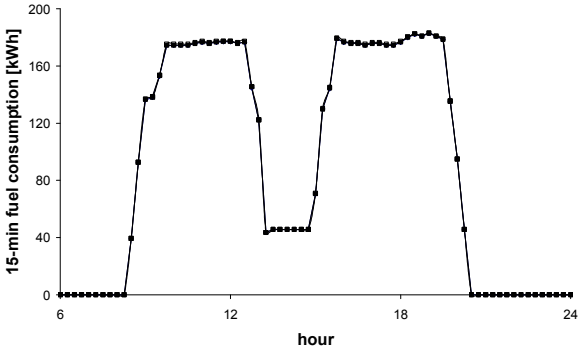

Fig. 13. Fuel consumption in the three optimization contexts (results are highly overlapped).

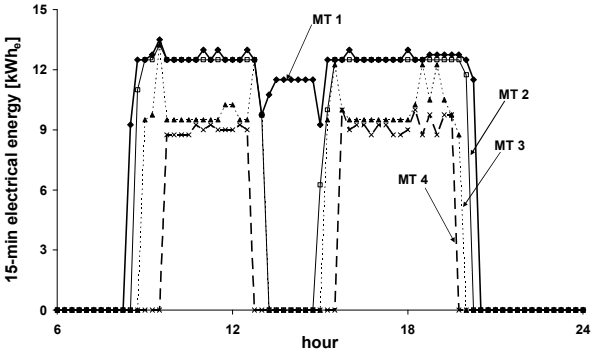

Fig. 14. MT usage with optimal NO_x emissions.

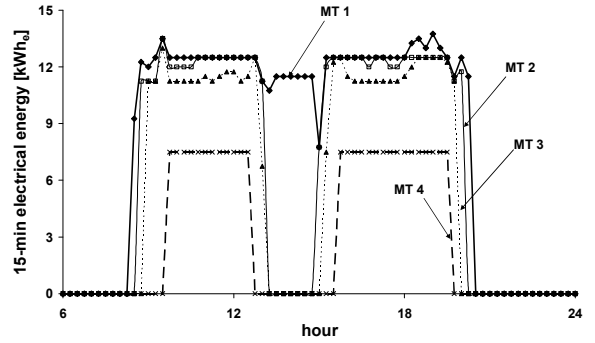

Fig. 15. MT usage with optimal CO emissions.

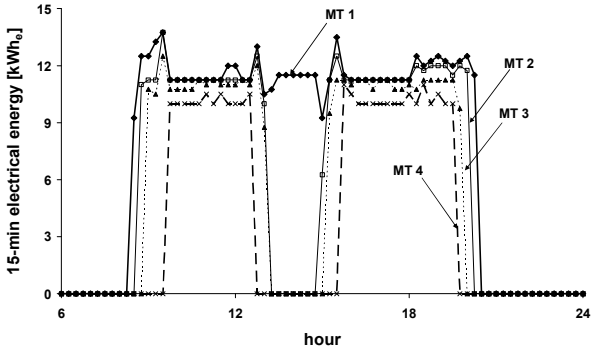

Fig. 16. MT usage with optimal fuel consumption.

C. Pareto analysis results

The results obtained from the optimization of the individual objectives are helpful to observe whether conflicting results arise from adopting the different objective functions. For the specific case with equal MT units, the solutions clearly tend to be similar when the hourly energy is slightly lower or equal to a multiple of the reference power. Conversely, with hourly energy values intermediate with respect to the multiples of the reference power, the presence of conflicting solutions is clearly visible. The best-known Pareto front has been calculated in these cases, by using the computational algorithm described in Section IV.B, with K = 100 chromosomes, crossover probability p_C = 0.6, mutation probability p_M = 0.1, stop criterion parameters ε = 0.1 and L = 20, and fitness multiplier ζ = 4. The results are represented in the *phenotype space* formed by the individual objective functions. Fig. 17 shows the resulting points for W_{TOT} = 120 kWh_e. These results indicate that the EA is able to find, in addition to the points A, B and C with minimum individual objectives, other non-dominated solutions representing compromise options for the multi-objective optimization problem. The numerical results are also reported in Table I, in order to check numerically that all these results correspond to non-dominated solutions.

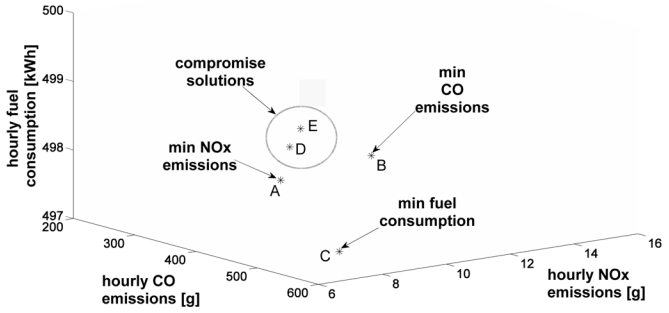

Fig. 17. Best-known Pareto front for W_{TOT} = 120 kWh_e.

TABLE I
HOURLY VALUES FOR THE POINTS OF THE BEST-KNOWN PARETO FRONT OF FIG. 17 (W_{TOT} = 120 kWh_e)

point	MT 1 [kWh_e]	MT 2 [kWh_e]	MT 3 [kWh_e]	MT 4 [kWh_e]	NOx [g]	CO [g]	Fuel [kWh]
A	50	35	35	0	**7.13**	479.3	498.1
B	45	45	30	0	14.19	**259.3**	497.5
C	42	40	38	0	8.54	501.5	**497.1**
D	49	36	35	0	7.45	477.6	498.6
E	50	36	34	0	8.26	453.2	498.8

The results reported in Fig. 17 and Table I refer to a single value of the total load. In order to get a broader picture, the best-known Pareto points are represented for values of W_{TOT} variable in the range 110÷220 kW_e, corresponding for instance to the range of interest for MT cluster operation at relatively high total load in the commercial centre case study. The representation has been split into three figures, in order to give the whole picture of the components of the objective array Z through three-dimensional views. The common part of these figures is the hourly energy axis. In the other axes, Fig. 18 presents the hourly CO emissions and the hourly fuel consumption, Fig. 19 reports the hourly NO_x emissions and the hourly fuel consumption, and Fig. 20 shows the hourly NO_x emissions and the hourly CO emissions. These figures give an overall picture of the impact of the objective functions (in particular the different behaviour of the specific NO_x and CO emissions at partial loads) on providing different optima and compromise solutions.

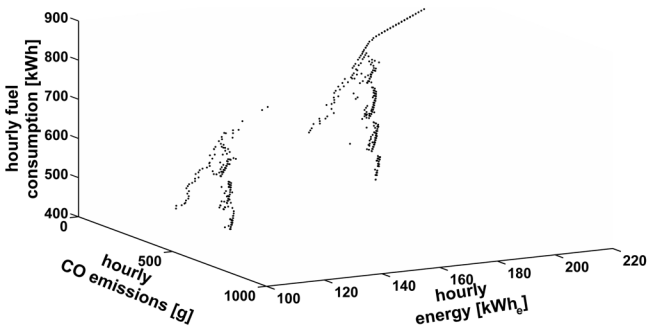

Fig. 18. Hourly CO emission and fuel consumption components of the best-known Pareto front for W_{TOT} variable from 110 to 220 kWh_e.

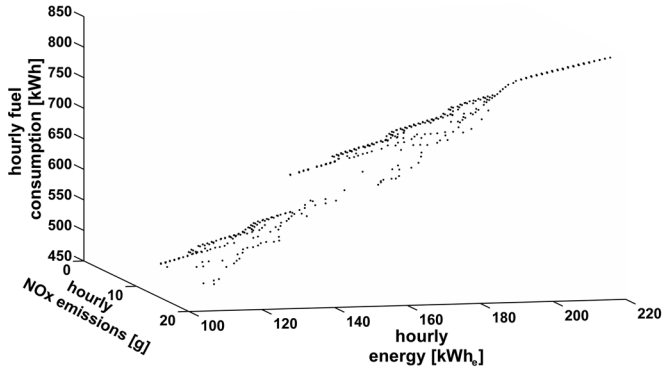

Fig. 19. Hourly NO_x emission and fuel consumption components of the best-known Pareto front for W_{TOT} variable from 110 to 220 kWh_e.

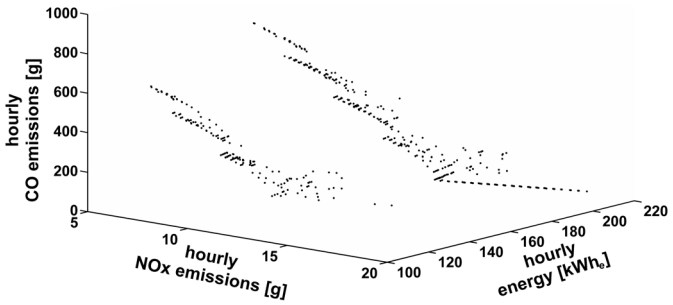

Fig. 20. Hourly NO_x and CO emission components of the best-known Pareto front for W_{TOT} variable from 110 to 220 kWh_e.

VI. CONCLUSIONS

Today's energy systems are more and more facing a plurality of objectives to be optimized, which calls for adequate multi-objective solution techniques. This paper has addressed the issues arising when considering the optimization of a cluster of MTs in load-following mode. Besides solving the individual optimizations with individual objectives to show to what extent they could be conflicting, a customized technique for determining the components of the best-known Pareto front has been introduced and discussed.

The results obtained in the case study by applying different optimization strategies have provided useful indications on the application of different operational strategies for the MT cluster. In particular, the MT usage patterns show that operation in pseudo-optimal conditions is possible without requiring excessive switch on/switch off operations during the day. On the other hand, the selection of the operational strategy has a significant impact on the emissions of the local pollutants, while it impacts less on the fuel consumption. The concepts illustrated can be applied to cases with higher number of MTs or different MT characteristics in a straightforward way. In this light, work in progress is aimed at generalizing the application of the approach discussed in this paper to address the energy efficiency, emission impact and economic assessment of combined local generation systems and of their interactions with the energy networks.

VII. References

[1] G. Chicco, P. Mancarella and R. Napoli, "Emission assessment of distributed generation in urban areas", *Proc. IEEE Power Tech 2007*, Lausanne, Switzerland, 1-5 July 2007.

[2] EDUCOGEN, The European Educational Tool on Cogeneration, December 2001, available: www.cogen.org/projects/educogen.htm.

[3] US Environmental Protection Agency (EPA), www.epa.org.

[4] A.Y. Petrov, A. Zaltash, T.D. Rizy and S.D. Labinov, "Environmental aspects of operation of a gas-fired microturbine-based CHP system", Oak Ridge National Laboratory report, 2001, available: http://www.ornl.gov/~webworks/cppr/y2001/pres/115331.pdf.

[5] Q. Yan, E.-S. Xu and Y.-P. Yang, "Pollutant Emission Reduction Analysis of Distributed Energy Resource", *Proc. 2nd International Conference on Bioinformatics and Biomedical Eng. (ICBBE 2008)*, Shanghai, China, 16-18 May 2008, 3839-3842.

[6] X. Pelet, D. Favrat and G. Leyland, "Multiobjective optimisation of integrated energy systems for remote communities considering economics and CO_2 emissions", *International Journal of Thermal Sciences* **44**, 2005, 1180–1189.

[7] T. Yalcinoz and O. Köskoy, "A multiobjective optimization method to environmental economic dispatch", *Electrical Power & Energy Systems* **29**, 2007, 42-50.

[8] J.P.S. Catalão, S.J.P.S. Mariano, V.M.F. Mendes and L.A.F.M. Ferreira, "Short-term scheduling of thermal units: emission constraints and trade-off curves", *European Transactions on Electr. Power* **18**, 2008, 1-14.

[9] K. Zehar and S. Sayah, "Optimal power flow with environmental constraint using a fast successive linear programming algorithm: Application to the Algerian power system", *Energy Conversion and Management* **49**, 2008, 3361–3365.

[10] X. Li, "Study of multi-objective optimization and multi-attribute decision-making for economic and environmental power dispatch", *Electric Power Syst. Research*, 2008, doi:10.1016/j.epsr.2008.10.016.

[11] J.H. Horlock, *Cogeneration - Combined Heat and Power*, Krieger, Malabar, FL, USA, 1997.

[12] A. Canova, G. Chicco and P. Mancarella, "Assessment of the Emissions due to Cogeneration Microturbines under Different Operation Modes", *Proc. Powereng 2007*, Setúbal, Portugal, April 2007, 684-689.

[13] G. Lozza, *Gas turbines and combined cycles* (in Italian), Progetto Leonardo, Bologna, Italy, 1996.

[14] D.E. Goldberg, *Genetic Algorithms in Search, Optimization and Machine Learning*, Addison-Wesley, 1989.

[15] A. Konak, D.W. Coir and A.E. Smith, "Multi-objective optimization using genetic algorithms: a tutorial", *Reliability Engineering and System Safety* **91**, 2006, 992-1007.

[16] P.K. Shukla and K. Deb, "On finding multiple Pareto-optimal solutions using classical and evolutionary generating methods", *European Journal of Operational Research* **181**, 2007, 1630-1652.

[17] D.E. Campbell and R. Nagahisa, "A foundation for Pareto aggregation", *Journal of Economic Theory* **64**, 1994, 277–285.

[18] K. Deb, A. Pratap, S. Agarwal and T. Meyarivan, "A fast and elitist multiobjective genetic algorithm: NSGA-II", *IEEE Trans. on Evolutionary Computation* **6** (2), April 2002, 182-197.

[19] A.-V. Boicea, G. Chicco and P. Mancarella, "Assessing the performance of microturbine clusters", *Proc. VII World Energy System Conference*, Iasi, Romania, June 30 - July 2, 2008.

VIII. Biographies

Adrian-Valentin Boicea (S'07) received the M.S. degree in Electrical Engineering and Electrical Power System from Universitatea Politehnica Bucuresti (UPB), Bucuresti, Romania, Fachbereich für Ingenieurwissenschaften, deutsche Abteilung, in 2006. Currently, he is an assistant professor of Electrical Measurement and Operations Research at UPB and PhD student at Politecnico di Torino, Italy. His research interests include the analysis of systems with distributed generation, energy efficiency, renewable sources, and applications of operational research techniques to the energy systems.

Gianfranco Chicco (M'98, SM'08) received the Ph.D. degree in Electrotechnical Engineering from Politecnico di Torino (PdT), Torino, Italy, in 1992. Currently, he is an Associate Professor of Electric Distribution Systems at PdT. His research interests include power system and distribution system analysis, competitive electricity markets, energy efficiency, load management, artificial intelligence applications, and power quality.

Pierluigi Mancarella (M'08) received the Ph.D. degree in Electrical Engineering from Politecnico di Torino (PdT), Torino, Italy, in 2006. Currently, he is a Research Associate at the Department of Electrical and Electronic Engineering, Imperial College London, UK. His research interests include distributed energy systems and energy networks, energy efficiency, and assessment of the environmental impact from energy generation.